energies

MDPI

Article

Multislot Simultaneous Spectrum Sensing and Energy Harvesting in Cognitive Radio

Xin Liu [1,3,*], Zhenyu Na [2], Min Jia [3,*], Xuemai Gu [3] and Xiaotong Li [2]

1 School of Information and Communication Engineering, Dalian University of Technology, Dalian 116024, China
2 School of Information Science and Technology, Dalian Maritime University, Dalian 116026, China; nazhenyu@dlmu.edu.cn (Z.N.); xtongli@yeah.net (X.L.)
3 Communication Research Center, Harbin Institute of Technology, Harbin 150080, China; guxuemai@hit.edu.cn
* Correspondence: liuxinstar1984@dlut.edu.cn (X.L.); jiamin@hit.edu.cn (M.J.); Tel.: +86-150-4051-1725 (X.L.); +86-136-1360-6260 (M.J.)

Academic Editor: Hongjian Sun
Received: 8 June 2016; Accepted: 15 July 2016; Published: 21 July 2016

Abstract: In cognitive radio (CR), the spectrum sensing of the primary user (PU) may consume some electrical power from the battery capacity of the secondary user (SU), resulting in a decrease in the transmission power of the SU. In this paper, a multislot simultaneous spectrum sensing and energy harvesting model is proposed, which uses the harvested radio frequency (RF) energy of the PU signal to supply the spectrum sensing. In the proposed model, the sensing duration is divided into multiple sensing slots consisting of one local-sensing subslot and one energy-harvesting subslot. If the PU is detected to be present in the local-sensing subslot, the SU will harvest RF energy of the PU signal in the energy-harvesting slot, otherwise, the SU will continue spectrum sensing. The global decision on the presence of the PU is obtained through combining local sensing results from all the sensing slots by adopting "Or-logic Rule". A joint optimization problem of sensing time and time splitter factor is proposed to maximize the throughput of the SU under the constraints of probabilities of false alarm and detection and energy harvesting. The simulation results have shown that the proposed model can clearly improve the maximal throughput of the SU compared to the traditional sensing-throughput tradeoff model.

Keywords: cognitive radio (CR); spectrum sensing; energy harvesting; throughput; detection probability

1. Introduction

To improve the current spectrum utilization, cognitive radio (CR) has been proposed to allow a secondary user (SU) to access the spectrum licensed to the primary user (PU), providing that the PU is not occupying the spectrum [1,2]. To avoid causing harmful interference to the PU, the SU should detect whether the PU exists in the frequency band depending on performing spectrum sensing before any available transmissions. Only if the absence of the PU is detected, can the SU access the PU spectrum for its transmission [3,4]. The spectrum sensing performance is reflected by the probabilities of false alarm and detection. Decreasing false alarm probability improves the spectrum access of the SU, while increasing detection probability reduces the interference to the PU [5].

Since it is often hard to obtain any PU information from the SU, energy sensing has been frequently used in CR as an effective spectrum sensing method, which can be implemented easily without acquiring any prior information from the emission signal of the PU [6]. Increasing sensing time may improve the sensing performance but decrease the transmission time, thus it is important to develop a

sensing-throughput tradeoff scheme to acquire both reliable energy sensing for detecting the presence of the PU signal and efficient data transmission for the SU [7]. In [8], the optimal sensing time is determined to maximize the achievable throughput of the SU subject to the constraint of detection probability of the PU. A joint optimization of sensing time and transmission power for maximizing the aggregate throughput of a cooperative CR network is studied in [9]. In [10], an energy-efficient CR system is designed to simultaneously meet spectrum sensing reliability and secondary data transmission rate constraints. However, the energy consumption for spectrum sensing, which may affect both energy sensing performance and transmission power of SU, has not been considered in [7–10]. The signal sampling of energy sensing has to consume some electrical power from the stored battery energy that originally supplies data transmission; thus, the achievable throughput of the SU is decreased.

Recently, energy harvesting has been proposed by some references, which may collect the radio frequency (RF) energy of the environmental signal sources to supply the electrical power for a wireless communication system instead of a fixed power supply [11,12]. An energy-harvesting circuit that consisted of semiconductor-based rectifying elements was designed to convert the received RF energy to the direct current (DC) power [13]. In [14,15], an energy-harvesting SU is investigated to harvest the RF energy of the PU signal in the transmission time when the PU is occupying this channel. However, energy harvesting is often performed independently after spectrum sensing; thus, the energy consumption of spectrum sensing cannot be duly supplemented. Moreover, since the spectrum sensing may consume some of the total power, without energy harvesting in the sensing duration, the initial transmission power of the SU may reduce, thus decreasing the transmission rate of the SU. Since the RF energy of the PU signal can be used both for spectrum sensing and energy harvesting, the simultaneous spectrum sensing and energy harvesting will become a profitable research are, which may save the consumed sensing energy by using the harvested PU signal energy to supply spectrum sensing.

The contributions of the paper are listed as follows:

- The paper firstly combines spectrum sensing and energy harvesting, the sensing duration is divided into multiple sensing slots consisted of one local-sensing subslot for energy sensing of the PU and one energy-harvesting subslot for harvesting the RF energy of the PU signal. If the presence of the PU is detected in the local-sensing subslot, the SU will harvest energy in the energy-harvesting subslot. Then the harvested energy is used to supply the spectrum sensing in the following sensing slot.
- The paper has proposed a jointly optimal allocation of sensing time and harvesting time to maximize the achievable throughput of the SU under the constraints that the target probabilities of detection and false alarm are both guaranteed and the harvested energy may supply the spectrum sensing. A joint optimization algorithm based on binary searching and alternating direction optimization (ADO) has been proposed to achieve the optimal solutions to the proposed optimization problem.

The rest of the paper is organized as follows: the energy sensing and energy harvesting are described in Section 2, both the system model building and the throughput of SU in the proposed model are given in Section 3, the joint optimization algorithm of sensing time and time splitting in the proposed model is defined in Section 4, and the simulations and discussions are finally drawn in Section 5.

2. Energy Sensing and Harvesting

2.1. Energy Sensing

Since SU and PU are two different kinds of communication systems, the SU is often hard to acquire any prior information of the PU signal, hence, energy detection is performed to sense the PU

as an effective spectrum sensing method, without needing any information of the detected signal. The detected signal y received by the SU is seen as a binary hypothesis problem as follows [16]:

$$y(t) = \begin{cases} n(t), H_0 \\ h(t)s(t) + n(t), H_1 \end{cases}, t = 1,\ 2,\ ...,\ M \tag{1}$$

where H_0 and H_1 denote the absence and presence of the PU, respectively, $s(t)$ is the PU signal with the power of p_s, $n(t)$ is the Gaussian noise with the variance of σ_n^2, $h(t)$ is the channel gain from the PU transmitter to the SU receiver, M is the number of the signal samples. We also suppose that $P(H_0)$ and $P(H_1)$ are the existent probabilities of H_0 and H_1, respectively. Supposing the sampling frequency as f_s and the sensing time as τ, we get $M = \tau f_s$. From Equation (1), the energy statistic of y is given as follows:

$$\Omega(y) = \frac{1}{M}\sum_{t=1}^{M} \|y(t)\|^2 \tag{2}$$

where $y(1), y(2), ..., y(M)$ are independently and identically distributed. With a large M, $\Omega(y)$ obeys the Gaussian distribution as follows:

$$\Omega(y) \sim \begin{cases} \mathcal{N}\left(\sigma_n^2, \frac{\sigma_n^4}{M}\right), H_0 \\ \mathcal{N}\left((1+\gamma)\,\sigma_n^2, \frac{(1+\gamma)^2\sigma_n^4}{M}\right), H_1 \end{cases} \tag{3}$$

where $\gamma = h^2 p_s / \sigma_n^2$ is the sensing signal to noise ratio (SNR). Comparing $\Omega(y)$ to a presettled detection threshold λ, the probabilities of false alarm and detection are respectively given as follows:

$$\begin{cases} P_f(\tau) = P_r\left(\Omega(y) \geq \lambda \,|H_0\right) = Q\left(\left(\frac{\lambda}{\sigma_n^2} - 1\right)\sqrt{\tau f_s}\right) \\ P_d(\tau) = P_r\left(\Omega(y) \geq \lambda \,|H_1\right) = Q\left(\left(\frac{\lambda}{\sigma_n^2(\gamma+1)} - 1\right)\sqrt{\tau f_s}\right) \end{cases} \tag{4}$$

where the function $Q(x) = \frac{1}{\sqrt{2\pi}}\int_x^{+\infty} \exp\left(-z^2/2\right) dz$.

2.2. Energy Harvesting

In this paper, we consider an energy-harvesting SU consisting of a spectrum sensing device and an energy-harvesting device, which converts the harvested RF energy of the PU signal to the electrical power for supplying spectrum sensing. The SU senses the PU signal and simultaneously stores the arriving energy from the PU in a rechargeable battery, through deploying an energy-harvesting circuit consisting of band-pass filter, rectifying circuit and low-pass filter, as shown in Figure 1.

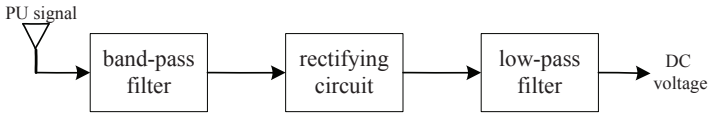

Figure 1. Energy-harvesting circuit. PU: primary user; and DC: direct current.

The SU firstly uses a band-pass filter to suppress the out-of-band energy radiation of the received PU signal and then converts the RF signal to a DC signal by the rectifying circuit. The rectifying circuit finally outputs the DC voltage after filtering out the fundamental and harmonic signals from the DC signal through a low-pass filter. However, some of the RF signal energy has to be reradiated to the outside environment due to the electromagnetic characters of the energy-harvesting circuit, thus we assume that $0 < \mu < 1$ is the energy-harvesting efficiency, which is determined by the characters of the energy-harvesting circuit elements [16].

3. System Model

3.1. Traditional Model

The traditional frame structure designed for the SU consists of one sensing slot and one data transmission slot, and the SU must firstly sense the absence of the PU before any available transmissions, as shown in Figure 2. We suppose the sensing duration as τ and the frame duration as T. The SU can operate in the frequency band of the PU in the following two scenarios [17]:

- When the PU is really absent in probability of $P(H_0)$ and no false alarm is generated by the SU in probability of $1 - P_f$, the SU may access the spectrum effectively in probability of $P(H_0)(1 - P_f)$;
- When the PU is really present in probability of $P(H_1)$ but not detected by the SU in probability of $1 - P_d$, the SU may also access the spectrum but cause harmful interference to the PU in probability of $P(H_1)(1 - P_d)$.

Thus, the average achievable throughput of the SU is given as follows:

$$R(\tau) = \frac{T - \tau}{T}\left(P(H_0)(1 - P_f(\tau))C_0 + P(H_1)(1 - P_d(\tau))C_1\right) \tag{5}$$

where C_0 and C_1 denote the throughput of the SU when it operates in the absence and presence of the PU, respectively. If there is only one point-to-point transmission in the secondary link, the SNR for this secondary link is $\gamma_{SU} = \frac{p_{SU} h_{SU}^2}{\sigma_n^2}$, where p_{SU} is the transmission power of the SU transmitter and h_{SU} is the channel gain from the SU transmitter to SU receiver. Then we have $C_0 = B \log_2(1 + \gamma_{SU})$ and $C_1 = B \log_2(1 + \frac{\gamma_{SU}}{1+\gamma})$ where B is the bandwidth, respectively. Obviously, we have $C_0 > C_1$.

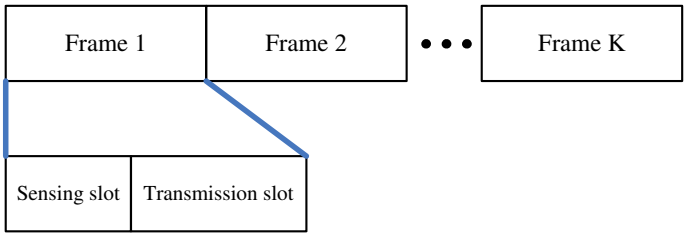

Figure 2. Traditional frame structure.

The higher the detection probability, the better the sensing performance. However, the lower the false alarm probability, the more chances the idle channel can be reused, thus the higher the throughput for the SU [18]. Thus there could exist a tradeoff between sensing performance and achievable throughput for the SU. The objective of sensing-throughput tradeoff model is to find the optimal sensing duration τ for maximizing the average throughput of the SU while the PU is sufficiently protected. Thus, the optimization problem of the sensing-throughput tradeoff model can be stated as follows [8]:

$$\max_{\tau} R(\tau) \tag{6a}$$

$$\text{s.t. } P_d(\tau) \geq \bar{P}_d \tag{6b}$$

where $\bar{P}_d$ is the lower limit of detection probability.

3.2. Proposed Model

In the common communication system, all the energy stored in the battery is used for data transmission. However, in CR system, the spectrum sensing has to consume some of the battery energy due to the circuit power of A/D chip and detector. Hence, the disadvantage of the traditional CR

system is that spectrum sensing has to consume some of the stored energy for data transmission, which decreases the transmission power and throughput of the SU transmitter compared with the common communication system. In this paper, we have proposed a multislot simultaneous spectrum sensing and energy harvesting model, where the sensing duration is further divided into N sensing slots, each of which consists of local-sensing subslot and energy-harvesting subslot, as shown in Figure 3. In each sensing slot, the SU firstly senses to make a local decision on the activity of the PU in the local-sensing subslot, then if the absence of the PU is detected, in case that the PU may suddenly appear later, the SU must continue sensing the PU in the energy-harvesting subslot and make a final decision at the end of the sensing slot. However, if the presence of the PU is detected accurately in the local-sensing subslot, the SU can harvest the RF energy of the PU signal in the energy-harvesting subslot. The harvested energy in the current sensing slot is used to supply the local spectrum sensing in the following sensing slot.

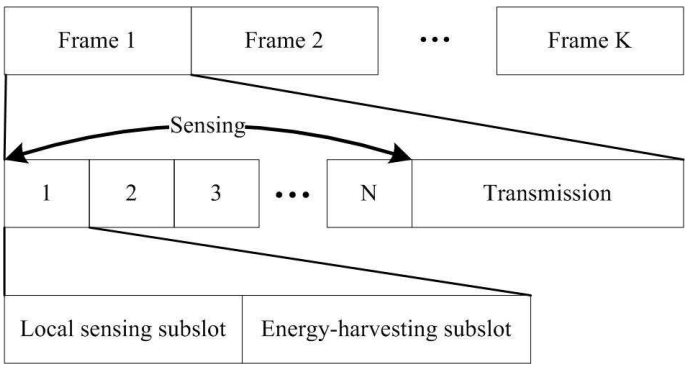

Figure 3. Proposed frame structure.

Supposing that the lengths of local-sensing subslot and energy-harvesting subslot are $\rho\tau$ and $(1-\rho)\tau$, respectively, where ρ is the time splitter factor, the probability of deciding the presence of the PU in the local-sensing subslot is $P(H_0)P_{\mathrm{f}}(\rho\tau) + P(H_1)P_{\mathrm{d}}(\rho\tau)$. However, the SU can harvest energy only when the PU is actually present, thus the harvested energy E_{H} in the energy-harvesting subslot is given by:

$$E_{\mathrm{h}}(\tau,\rho) = \mu P(H_1)P_{\mathrm{d}}(\rho\tau)p_{\mathrm{s}}h^2(1-\rho)\tau \tag{7}$$

While the probability of deciding the absence of the PU in the local-sensing subslot is $\xi = P(H_0)(1-P_{\mathrm{f}}(\rho\tau)) + P(H_1)(1-P_{\mathrm{d}}(\rho\tau))$. If the absence of the PU is detected, the SU must sense the PU both in local-sensing subslot and energy-harvesting subslot in probability of ξ, thus the average sensing time is $\rho\tau + \xi(1-\rho)\tau$. The achieved probabilities of false alarm and detection at the end of the sensing slot is $P_{\mathrm{f}}(\rho\tau + \xi(1-\rho)\tau)$ and $P_{\mathrm{d}}(\rho\tau + \xi(1-\rho)\tau)$. At the end of the sensing duration, the SU will obtain a global decision on the activity of the PU through combining these sensing results from all the sensing slots by adopting "Or-logic Rule". Thus the global probabilities of false alarm and detection are given as follows:

$$\begin{cases} P_{\mathrm{f}}^{\mathrm{g}}(\tau,\rho) = 1 - \left(1 - P_{\mathrm{f}}\big(\rho\tau + \xi(1-\rho)\tau\big)\right)^N \\ P_{\mathrm{d}}^{\mathrm{g}}(\tau,\rho) = 1 - \left(1 - P_{\mathrm{d}}\big(\rho\tau + \xi(1-\rho)\tau\big)\right)^N \end{cases} \tag{8}$$

The average number of sampling nodes in each sensing slot is $\big(\rho\tau + \xi(1-\rho)\tau\big)f_s$. Supposing the unit sampling energy as e_{s}, the total spectrum sensing energy is $E_{\mathrm{s}} = Ne_{\mathrm{s}}\big(\rho\tau + \xi(1-\rho)\tau\big)f_{\mathrm{s}}$. In case that the PU is not present in the whole sensing duration, we assume that the minimal energy for spectrum sensing supported by the battery is E_{m} and thus have $NE_{\mathrm{h}} + E_{\mathrm{m}} \geq E_{\mathrm{s}}$. In fact, the harvested energy NE_{h} is used to compensate the loss of transmission power of the SU, thus supposing

$\tau \ll T$, the compensated transmission power $\triangle p_{SU} \approx \frac{NE_h}{T}$. The compensated SNR for the secondary link is $\triangle \gamma_{SU} = \frac{\triangle p_{SU} h_{SU}^2}{\sigma_n^2}$, thus the throughput of the SU in the absence and presence of the PU are $\tilde{C}_0 = \log_2(1 + \gamma_{SU} + \triangle \gamma_{SU})$ and $\tilde{C}_1 = \log_2(1 + \frac{\gamma_{SU} + \triangle \gamma_{SU}}{1+\gamma})$, respectively.

Like Equation (5), substituting Equation (8), the average throughput of the SU in the proposed model is given as follows:

$$\tilde{R}(\tau, \rho) = \frac{T - N\tau}{T} \times \left(P(H_0)(1 - P_f^g(\tau, \rho))\tilde{C}_0 + P(H_1)(1 - P_d^g(\tau, \rho))\tilde{C}_1 \right) \tag{9}$$

When there is no any transmissions in CR, the maximal lifetime of the traditional CR network can be obtained by:

$$LT = \frac{E_T}{e_s f_s} \tag{10}$$

where E_T is the total battery energy. However, according to Equation (7), the maximal lifetime of the energy-harvesting CR network can be given by:

$$\tilde{LT} = \frac{E_T}{e_s f_s - \mu P(H_1) P_d p_s h^2} \tag{11}$$

where obviously, $\tilde{LT} > LT$.

4. Model Optimization

In the proposed system model, our goal is to maximize the average achievable throughput of the SU through jointly optimizing sensing time τ and time splitter factor ρ, subject to the constraints that the probabilities of detection and false alarm are both guaranteed and the harvested energy may supply the spectrum sensing, as follows:

$$\max_{\tau, \rho} \tilde{R}(\tau, \rho) \tag{12a}$$

$$\text{s.t. } P_d^g(\tau, \rho) \geq \bar{P}_d, P_f^g(\tau, \rho) \leq \bar{P}_f \tag{12b}$$

$$NE_h + E_m \geq E_s \tag{12c}$$

$$0 \leq \tau \leq \frac{T}{N} \tag{12d}$$

$$0 \leq \rho \leq 1 \tag{12e}$$

where P_f is the upper limit of false alarm probability. We use ADO to solve Equation (12) [19]. Firstly, we fix $\rho = \rho_0$ where $\rho_0 \in (0, 1)$ and optimize τ. Then from Equation (4), since $Q(x)$ is a monotonously decreasing function, P_f and P_d have the same monotonicity in τ and thus from Equation (8), P_f^g increases as P_d^g improves. Thus from Equation (9), $\tilde{R}$ reduces with the increasing of P_d^g, i.e., $\tilde{R}$ may achieve the maximum only if P_d^g acquires its lower bound as $P_d^g = \bar{P}_d$. Then from Equations (4) and (8), P_f^g is related to $\bar{P}_d$ as follows:

$$P_f^g = 1 - \left(1 - Q\left(Q^{-1}\left(1 - (1 - \bar{P}_d)^{\frac{1}{N}}\right)(\gamma + 1) + \gamma \sqrt{(\rho_0 \tau + \xi(1 - \rho_0)\tau) f_s}\right)\right)^N \tag{13}$$

With $P_f^g \leq \bar{P}_f$ and $P_d^g = \bar{P}_d$, we have $\xi \geq P(H_0)(1 - \bar{P}_f)^{\frac{1}{N}} + P(H_1)(1 - \bar{P}_d)^{\frac{1}{N}}$. From Equation (13), P_f^g decreases as ξ increases and thus we may optimize Equation (12) using $\xi = P(H_0)(1 - \bar{P}_f)^{\frac{1}{N}} + P(H_1)(1 - \bar{P}_d)^{\frac{1}{N}}$. Substituting Equation (7) into Equation (12c), it is obtained that:

$$\tau \leq \tau_h \text{ where } \tau_h = \frac{E_m}{N(\eta_1 \rho_0 + (1 - \rho_0)(\eta_1 \xi - \eta_0))} \tag{14}$$

where $\eta_0 = \mu P(H_1)\bar{P}_d p_s h^2$ and $\eta_1 = e_s f_s$. Then from $P_f^g \le \bar{P}_f$, we get that:

$$\tau \ge \tau_l \text{ where } \tau_l = \frac{\left(Q^{-1}(\bar{P}_f) - Q^{-1}(1-(1-\bar{P}_d)^{\frac{1}{N}})(\gamma+1)\right)^2}{\gamma^2 f_s\left(\rho_0 + \xi(1-\rho_0)\right)} \tag{15}$$

Substituting Equations (13) and (14) into Equation (12), with given ρ_0, the optimization problem of τ is simply rewritten as follows:

$$\max_{\tau} \tilde{R}(\tau) = \frac{T - N\tau}{T}\left(\varphi_0(1 - Q(\omega_0 + \gamma\sqrt{\omega_1 \tau f_s}))^N + \varphi_1\right) \tag{16a}$$

$$\text{s.t. } \tau_l \le \tau \le \min\left\{\frac{T}{N}, \tau_h\right\} \tag{16b}$$

where $\omega_0 = Q^{-1}\left(1-(1-\bar{P}_d)^{\frac{1}{N}}\right)(\gamma+1)$, $\omega_1 = \rho_0 + \xi(1-\rho_0)$, $\varphi_0 = P(H_0)\tilde{C}_0$ and $\varphi_1 = P(H_1)(1-\bar{P}_d)\tilde{C}_1$. Then we express that there exists an optimal solution $\tau_z \in \left(0, \frac{T}{N}\right)$ to make $\tilde{R}(\tau)$ achieve the maximum. Take the first-order derivative of Equation (16a) in τ as follows:

$$\begin{aligned} \nabla\tilde{R}(\tau) = &-\frac{N}{T}\left(\varphi_0(1 - Q(\omega_0 + \gamma\sqrt{\omega_1\tau f_s}))^N + \varphi_1\right) + \\ &\frac{N\varphi_0\gamma(T - N\tau)\sqrt{\omega_1 f_s}}{2T\sqrt{2\pi\tau}}\left(1 - Q(\omega_0 + \gamma\sqrt{\omega_1\tau f_s})\right)^{N-1} e^{-\frac{(\omega_0 + \gamma\sqrt{\omega_1\tau f_s})^2}{2}} \end{aligned} \tag{17}$$

Noting $0 < Q(x) < 1$, we deduce the limit values from Equation (17) as follows:

$$\begin{cases} \lim\limits_{\tau\to 0} \nabla\tilde{R}(\tau) \approx \frac{N\varphi_0\gamma T\sqrt{\omega_1 f_s}}{2T\sqrt{2\pi\tau}}\left(1 - Q(\omega_0)\right)^{N-1} e^{-\frac{\omega_0^2}{2}} \to +\infty \\ \lim\limits_{\tau\to\frac{T}{N}} \nabla\tilde{R}(\tau) < -\frac{N}{T}\left(\varphi_0(1 - Q(\omega_0))^N + \varphi_1\right) < 0 \end{cases} \tag{18}$$

which indicates that there exists a $\tau_z \in \left(0, \frac{T}{N}\right)$ to make $\nabla\tilde{R}(\tau) = 0$. Equation (18) also means that $\nabla\tilde{R}(\tau)$ increases when τ approaches 0 and decreases when τ approaches $\frac{T}{N}$. Hence, there is a maximum point τ_z of $\tilde{R}(\tau)$ within interval $(0, \frac{T}{N})$. τ_z can be obtained through the Algorithm 1 based on the binary searching.

Algorithm 1: Searching algorithm of $\tau_z \in \left(0, \frac{T}{N}\right)$ for maximizing $\tilde{R}(\tau)$

(1) Initialize $\tau_{min} = 0$, $\tau_{max} = \frac{T}{N}$ and estimation error δ;
(2) While $(|\tau_{max} - \tau_{min}| > \delta)$ do:
(3) Set $\tau_z = \frac{\tau_{min} + \tau_{max}}{2}$;
(4) If $(\nabla\tilde{R}(\tau_z) == \nabla\tilde{R}(\tau_{min}))$: set $\tau_{min} = \tau_z$;
(5) Else if $(\nabla\tilde{R}(\tau_z) == \nabla\tilde{R}(\tau_{max}))$: set $\tau_{max} = \tau_z$;
(6) End if;
(7) End while;
(8) Output $\tau_z = \frac{\tau_{min} + \tau_{max}}{2}$.

Noting $\tau_l \le \tau \le \min\left\{\frac{T}{N}, \tau_h\right\}$ and $\tau_z < \frac{T}{N}$, we may get $\tau_l \le \tau \le \min\{\tau_z, \tau_h\}$. Thus the optimal τ^* to solve Equation (16) is given as follows:

$$\tau^* = \max\left\{\tau_l,\ \min\{\tau_z, \tau_h\}\right\} \tag{19}$$

Secondly, we fix $\tau_0 = \tau^*$ and optimize ρ. From Equation (12c), with given τ_0, the upper limit of ρ is obtained as follows:

$$\rho \leq \frac{\frac{E_m}{N\tau_0} + \eta_0 - \eta_1\xi}{\eta_1(1-\xi)+\eta_0} \tag{20}$$

As seen from Equation (13), P_f^g decreases monotonously as ρ increases, i.e., the throughput $\tilde{R}$ may achieve the maximum only if ρ acquires its upper limit as $\rho = \min\{1, \frac{\frac{E_m}{N\tau_0}+\eta_0-\eta_1\xi}{\eta_1(1-\xi)+\eta_0}\}$. Using ADO, the joint optimal solutions (τ^*, ρ^*) to Equation (12) are obtained, through iteratively and alternately optimizing τ and ρ until both of them are convergent, as shown in Algorithm 2. Since the existent convergence of τ has been expressed as above, we can also get the convergence of ρ that is uniquely determined by τ. Noting that the locally optimal value in each iteration k is non-decreasing, we can get $\tilde{R}(\tau^{(k-1)}, \rho^{(k-1)}) \leq \tilde{R}(\tau^{(k)}, \rho^{(k-1)}) \leq \tilde{R}(\tau^{(k)}, \rho^{(k)})$, which indicates that the convergence of $\tilde{R}$ can be obtained if τ and ρ are both convergent.

Algorithm 2: Joint optimization algorithm

(1) initialize $k = 0$, $\tau^{(k)} = 0$, $\rho^{(k)} = \rho_0$ where $\rho_0 \in (0, 1)$ and estimation error δ;
(2) with given $\rho^{(k)}$, calculate τ^* according to Algorithm 1 and Equation (19);
(3) set $\tau^{(k+1)} = \tau^*$;
(4) with given $\tau^{(k+1)}$, calculate $\rho^* = \min\{1, \frac{\frac{E_m}{N\tau^{(k+1)}}+\eta_0-\eta_1\varepsilon}{\eta_1(1-\varepsilon)+\eta_0}\}$;
(5) set $\rho^{(k+1)} = \rho^*$ and $k = k - 1$;
(6) repeat (2)-(5) until both $|\tau^{(k)} - \tau^{(k-1)}| \leq \delta$ and $|\rho^{(k)} - \rho^{(k-1)}| \leq \delta$ are satisfied.

The time complexity of the binary searching in Algorithm 1 is $O(\log \frac{T}{N\delta})$ and the iterative number of the Algorithm 2 is $O(\frac{1}{\delta^2})$. Noting that the Algorithm 1 is implemented once in each iteration of Algorithm 2, the total time complexity is $O(\frac{1}{\delta^2} \log \frac{T}{N\delta})$. To describe the energy harvesting performance, we define the energy-harvesting efficiency as follows:

$$\theta = \frac{\triangle R}{E_h} \tag{21}$$

where $\triangle R$ is the throughput increment between energy-harvesting SU and non-energy-harvesting SU.

5. Simulations and Discussion

In the simulations, we suppose that the frame duration $T = 20$ ms, the number of sensing slots $N = 5$, the probabilities of H_0 and H_1 are $P(H_0) = P(H_1) = 0.5$, respectively, the sampling frequency $f_s = 1$ MHz, the channel gain h obeys the Rayleigh distribution with the mean of -10 dB, the bandwidth B = 1 KHz, the PU power $p_s = 10$ dBW, the SU power p_{SU} = 10 dBW, the noise variance σ_n^2 = 1 dBW, the unit sampling energy e_s = 0.1 mJ and the minimum spectrum sensing energy supported by the battery E_m = 10 mJ.

Figure 4 shows the global false alarm probability P_f^g of the proposed sensing model versus the time splitter factor $\rho = \{0.1, 0.3, 0.5, 0.7\}$, with different global detection probability P_d^g. It is seen that P_f^g and P_d^g have the same monotonicity, which indicates that the spectrum access decreases as P_d^g improves and the maximal throughput can be obtained if P_d^g acquires its lower limit; P_f^g decreases as ρ increases, which indicates that the maximal spectrum access can be achieved if ρ acquires its upper limit. Figure 5 indicates the throughput R changed with the sensing time τ. It is seen that there exists an optimal τ that makes R achieve the maximum. When τ is small, R improves as τ increases, because the spectrum sensing performance mainly improves; however, when τ is large, R decreases as τ increases, because the data transmission time mainly decreases. Thus, there is a tradeoff between spectrum sensing and throughput.

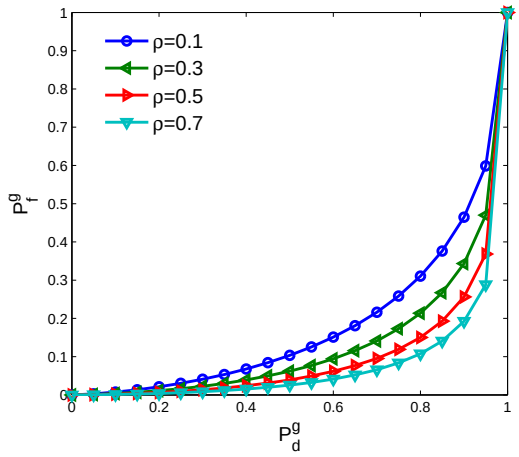

Figure 4. Global false alarm probability versus time splitter factor.

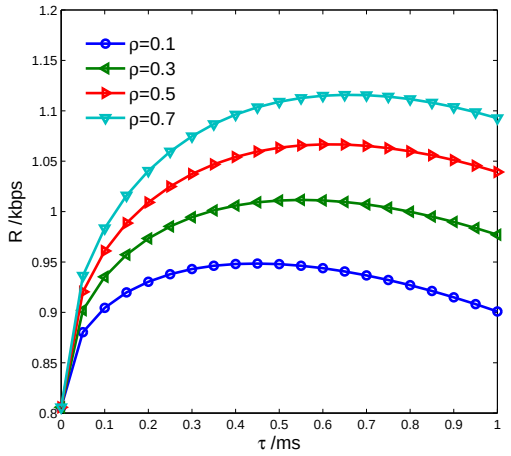

Figure 5. Throughput changed with sensing time.

Figure 6 shows the throughput R changed with the harvested energy E_{h} with $P_{\mathrm{d}}^{\mathrm{g}} = \{0.75, 0.8, 0.85, 0.9\}$. It is seen that R decreases as E_{h} increases, because the sensing time decreases while the harvesting time increases, which yields higher false alarm probability but more harvested energy. Thus the larger throughput can be achieved if the harvested energy appropriately supplies the spectrum sensing.

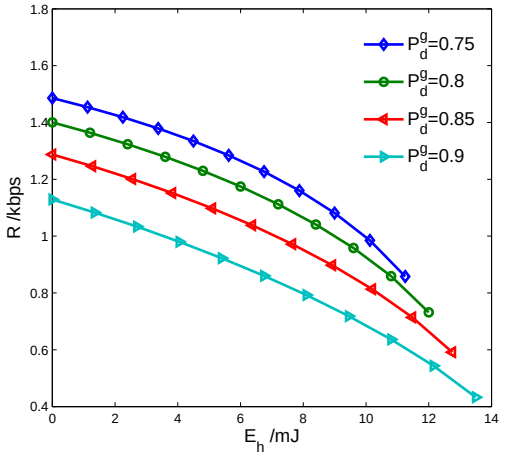

Figure 6. Throughput changed with harvested energy.

Figure 7 indicates the throughput versus different spectrum sensing models: the traditional sensing-throughput tradeoff model [8] and the proposed simultaneous spectrum sensing and energy harvesting model with $\rho = \{0.1, 0.3, 0.5\}$. It is seen that the throughput of the traditional model is larger than that of the proposed model with $\rho = \{0.1, 0.3\}$, because the spectrum sensing performance is very low with small ρ and the false alarm probability is very large; however, the throughput of the traditional model is smaller than that of the proposed model with large ρ, because the lost transmission energy is compensated with the harvested energy while the spectrum sensing performance is guaranteed.

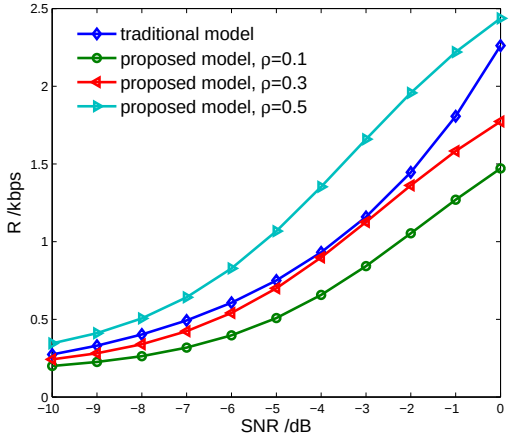

Figure 7. Throughput versus spectrum sensing models. SNR: signal to noise ratio.

Figure 8 indicates the maximum throughput versus theoretic optimum and joint optimum with $P_{\mathrm{d}}^{g} = \{0.75, 0.8, 0.85, 0.9\}$. It is seen that the maximal throughput obtained by the joint optimization algorithm accords with the corresponding theoretical maximum.

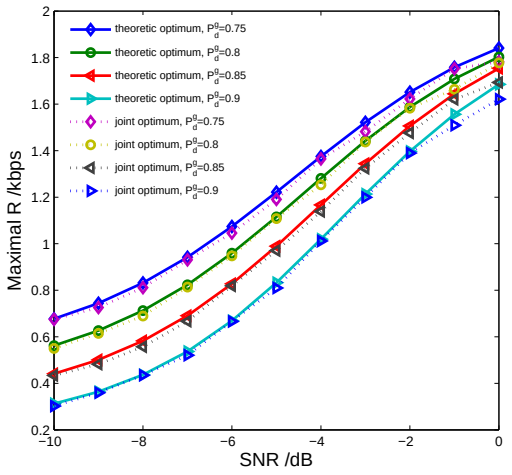

Figure 8. Maximal throughput versus theoretic optimum and joint optimum.

Figure 9 shows the maximum throughput versus different spectrum sensing models: the traditional sensing-throughput tradeoff model [8] and the proposed model. It is seen that the proposed model can improve the achievable maximal throughput of the SU obviously through using the harvested energy of the PU signal to compensate the energy consumption of spectrum sensing. Figure 10 indicates the energy-harvesting efficiency θ versus traditional energy-harvesting SU [15] and the proposed energy-harvesting SU, with different frame duration T. It is seen that the efficiency of the traditional SU is lower than that of the proposed SU under small T but higher under large T, because the traditional SU can only harvest energy in the transmission slot and the sensing energy

consumption cannot be supplemented. Figure 11 compares the lifetime of the tradiotnal CR and the energy-harvesting CR. It is seen that the energy-harvesting CR can achieve longer life.

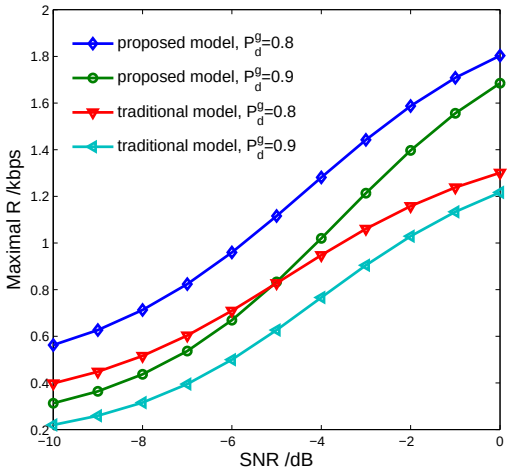

Figure 9. Maximal throughput versus spectrum sensing models.

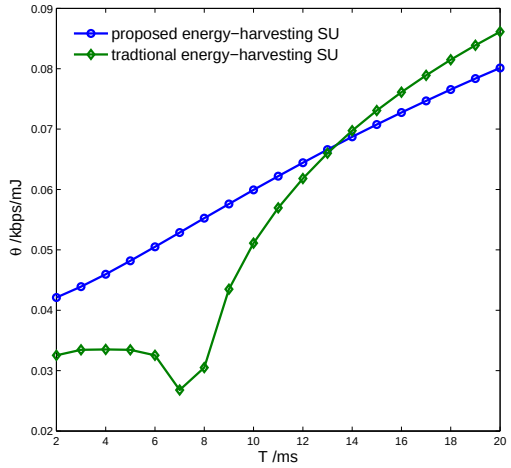

Figure 10. Energy-harvesting efficiency versus frame duration. SU: secondary user.

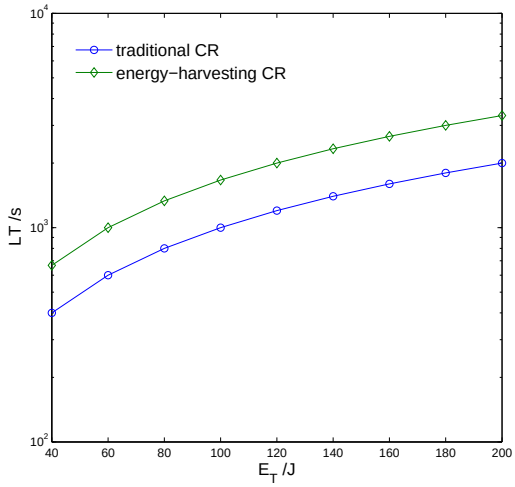

Figure 11. Lifetime comparison of different cognitive radio (CR) systems.

6. Conclusions

In this paper, a multislot simultaneous spectrum sensing and energy harvesting model is proposed to improve the achievable throughput of the SU through using the harvested RF energy of the PU signal to compensate the energy consumption of spectrum sensing. The sensing duration is divided into multiple sensing slots, each of which consisted of one local-sensing subslot for energy sensing and one energy-harvesting subslot for collecting the RF energy in the presence of the PU. We have formulated a joint optimization problem of sensing time and time splitter factor to maximize the average achievable throughput of the SU. From the simulations, we have concluded the following results:

- there exists an optimal sensing time that maximizes the average achievable throughput of the SU while the sensing performance is guaranteed;
- the maximal throughput of the SU can be obtained only if the detection probability acquires its lower limit and the harvested energy appropriately supplies spectrum sensing;
- the proposed model can improve the maximal throughput of the SU obviously through using the harvested energy to compensate the energy consumption of spectrum sensing.

In the future, we will apply the proposed model in cooperative spectrum sensing.

Acknowledgments: This work was supported by the National Natural Science Foundations of China under Grant Nos. 61301131 and 91438205, the Natural Science Foundation of Jiangsu Province under Grant No. BK20140828, the Fundamental Research Funds for the Central Universities under Grant No. DUT16RC(3)045, the Chinese Postdoctoral Science Foundation under Grant No. 2015M580425, the Scientific Research General Project of Liaoning Province Eduction Commission under Grant No. L2014204.

Author Contributions: Xin Liu and Zhenyu Na conceived and designed the communication models; Min Jia and Xuemai Gu optimized the proposed models; Xiaotong Li performed the simulations of the model; Xin Liu wrote the paper.

Conflicts of Interest: The authors declare no conflict of interest.

References

1. Hamdaoui, B. Adaptive spectrum assessment for opportunistic access in cognitive radio networks. *IEEE Trans. Wirel. Commun.* **2009**, *8*, 922–930.
2. Haykin, S. Cognitive radio: Brain-empowered wireless communications. *IEEE J. Sel. Areas Commun.* **2005**, *23*, 201–220.
3. Liu, X.; Tan, X. Optimization algorithm of periodical cooperative spectrum sensing in cognitive radio. *Int. J. Commun. Syst.* **2014**, *27*, 705–720.
4. Sun, H.; Nallanathan, A.; Wang, C.; Chen, Y. Wideband spectrum sensing for cognitive radio networks: A survey. *IEEE Wirel. Commun.* **2013**, *20*, 74–81.
5. Liu, X.; Bi, G.; Jia, M.; Guan, Y.L.; Zhong, W.; Lin, R. Joint optimization of sensing threshold and transmission power in wideband cognitive radio. *Radio Sci.* **2013**, *48*, 359–370.
6. Shen, J.; Liu, S.; Wang, Y.; Xie, G.; Rashvand, H.F.; Liu, Y. Robust energy detection in cognitive radio. *IET Commun.* **2009**, *3*, 1016–1023.
7. Tang, L.; Chen, Y.; Hines, E.L.; Alouini, M.S. Effect of primary user traffic on sensing-throughput tradeoff for cognitive radios. *IEEE Trans. Wirel. Commun.* **2011**, *10*, 1063–1068.
8. Liang, Y.; Zeng, Y.; Peh, E.C.Y, Hoang, A.T. Sensing-throughput tradeoff for cognitive radio networks. *IEEE Trans. Wirel. Commun.* **2008**, *7*, 1326–1337.
9. Liu, X. A new sensing-throughput tradeoff scheme in cooperative multiband cognitive radio network. *Int. J. Netw. Manag.* **2014**, *24*, 200–217.
10. Subhankar, C.; Santi, P.M.; Tamaghna, A. Energy efficient cognitive radio system for joint spectrum sensing and data transmission. *IEEE J. Emerg. Sel. Top. Circuits Syst.* **2014**, *4*, 292–300.
11. Valenta, C.R.; Durgin, G.D. Harvesting wireless power: survey of energy-harvester conversion efficiency in farfield, wireless power transfer systems. *IEEE Microw. Mag.* **2014**, *15*, 108–120.
12. Liu, L.; Zhang, R.; Chua K.C. Wireless information transfer with opportunistic energy harvesting. *IEEE Trans. Wirel. Commun.* **2013**, *3*, 345–362.

13. Ren, Y.; Li, M.; Chang, K. 35 GHz rectifying antenna for wireless power transmission. *Electron. Lett.* **2007**, *43*, 602–603.
14. Lee, S.; Zhang, R.; Huang, K. Opportunistic wireless energy harvesting in cognitive radio networks. *IEEE Trans. Wirel. Commun.* **2013**, *12*, 4788–4799.
15. Ding, T.H.; Niyato, D.; Wang, P.; Kim, D.I. Opportunistic channel access and RF energy harvesting in cognitive radio networks. *IEEE J. Sel. Areas Commun.* **2014**, *32*, 2039–2052.
16. Liu, X.; Chen, K.; Yan, J.; Na, Z.Y. Optimal energy harvesting-based weighed cooperative spectrum sensing in cognitive radio network. *Mobile Netw. Appl.* **2016**, *3*, 1–12.
17. Liu, X.; Jia, M.; Gu, X.; Tan, X. Optimal periodic cooperative spectrum sensing based on weight fusion in cognitive radio networks. *Sensors* **2013**, *13*, 5251–5272.
18. Gou, K.; Sun, L.; LI, Y.; Jia, S. Channel-aware and queue-aware joint-layer resource optimization for cognitive radio networks. *Sci. China Inf. Sci.* **2010**, *53*, 2576–2583.
19. Boyd, S.; Parikh, N.; Chu, E.; Peleato, B.; Eckstein, J. Distributed optimization and statistical learning via the alternating direction method of multipliers. *Found. Trends Mach. Learn.* **2011**, *3*, 1–122.